Journal of Marine Science and Technology

Volume 16 | Issue 1 Article 8

PROFILE DESIGN OF PISTON RING USING INVERSE METHOD

Li-Ming Chu
Department of Mechanical and Automation Engineering, I-Shou University, Kaohsiung County 840, Taiwan, R.O.C., hmchu@mail.isu.edu.tw

Yuh-Ping Chang
Department of Mechanical Engineering, Kun Shan University, Tainan 710, Taiwan, R. O. C.

Jung-Hua Yang
Department of Vehicle Engineering, National Pingtung University of Science and Technology, Ping-Tung 912, Taiwan, R.O.C.

PROFILE DESIGN OF PISTON RING USING INVERSE METHOD

Acknowledgements

The authors would like to express their appreciation to the National Science Council (NSC-95-2221-E-132-003) in Taiwan for financial support.

PROFILE DESIGN OF PISTON RING USING INVERSE METHOD

Li-Ming Chu*, Yuh-Ping Chang**, and Jung-Hua Yang***

Key words: piston ring profile, inverse method, pressure distribution.

ABSTRACT

This study aims to develop an algorithm for designing the piston ring profile and pressure distribution using an inverse method. The proposed algorithm needs to obtain load and boundary conditions for estimating not only a smooth curve in the piston ring profile, but also in the pressure distribution. The algorithm is developed from Reynolds integral and force balance equations. The least-squares error method, variational method, Gauss-Seidel method and Newton-Raphson method are employed to calculate the piston ring profile. Simulation results reveal that the greater the degree of the polynomial function used, the greater the maximum pressure ($P_{\max}$), load and friction coefficient are, and the smaller the minimum film thickness ($H_{\min}$) is. However, as the degree of the polynomial function and the number of grid points increase, the estimated piston ring profile and pressure distribution become more accurate. The initial guessed values of the coefficients of the estimated piston ring profile (C_j) and the position of maximum pressure (X_m) have more obvious effects upon the present algorithm. The initial guessed value of C_j can allow greater error than that of X_m when estimating $P_{\max}$ and $H_{\min}$ using the present algorithm. Consequently, the present algorithm is capable of providing accurate results in terms of piston ring profile and pressure distribution.

I. INTRODUCTION

It is well known that effective sealing between piston rings and cylinder liners ensure successful operation of reciprocating engines. However, the friction power loss caused by the piston rings makes up a large proportion of the power loss of the internal combustion engine (approximately 20 percent to 40 percent). Therefore, an understanding of the necessity of lubrication between piston rings and the cylindrical wall is vital for reducing engine friction. Hence, designing a profile of piston ring with a good lubrication condition that can reduce frictional losses between the piston ring and the cylinder liner is a key technology in the design of internal combustion engines.

Hawkers and Hardy [9] found that hydrodynamic lubrication (HL) prevailed throughout most of the engine cycle by friction measurements. They first proposed the evidence of hydrodynamic lubrication between a piston ring and a cylinder liner in 1936. Castleman [1] applied the concept of hydrodynamic lubrication to piston ring analysis. Eilon and Saunders [5] assumed a symmetric parabolic profile, and calculated the thickness of the oil film and the friction force of the ring. Furuhama [6] considered a ring profile consisting of a central flat region and two circular arcs at the two ends. He took into account the variations in pressure and speed throughout the cycle, which create the squeeze film effect. Ting and Mayer [14] analyzed the blow by gas pressure between the rings in a piston ring pack, as well as ring lubrication and cylinder bore wear. Dowson *et al.* [3] used a hydrodynamic lubrication model with the Reynolds boundary condition to study piston ring lubrication. The effect of oil starvation was considered in their model. Jeng [11] developed a one-dimensional analysis for lubrication between a piston ring and a cylinder liner to explore the effects of ring profile, ring tension, and engine speed. This analysis can be used for studying the influence of ring design parameters in reciprocating engines. Hwu and Weng [10] used a non-linear finite element scheme, employing the Newton-Raphson-Murty algorithm to analyze the problem of elastohydrodynamic lubrication (EHL) of piston rings. In order to converge quickly, Wu and Chen [15] applied the multigrid method to analyze the EHL problem of piston rings. Further, Dowson *et al.* [4] also investigated piston ring lubrication and proposed strong EHL effects near the top dead center (TDC). In particular, the EHL theory has been more suitably adopted to predict the results at the beginning of a combustion cycle.

When assessing the effectiveness of a lubricant, it is important to measure the thickness of the film in the piston ring and cylinder liner. Takiguchi *et al.* [12] measured the friction forces up to an engine speed of 5000rpm using measuring instruments for piston friction forces in order to clarify the friction forces and conditions of lubrication at high engine speeds. Their results showed that piston friction is mainly caused by hydrodynamic lubrication at high engine speeds above 2500rpm in the

Paper submitted 10/23/06; accepted 03/27/07. Author for correspondence: Li-Ming Chu (e-mail: hmchu@mail.isu.edu.tw).
** Department of Mechanical and Automation Engineering, I-Shou University, Kaohsiung County 840, Taiwan, R.O.C.*
*** Department of Mechanical Engineering, Kun Shan University, Tainan 710, Taiwan, R. O. C.*
**** Department of Vehicle Engineering, National Pingtung University of Science and Technology, Ping-Tung 912, Taiwan, R.O.C.*

test engine. Furuhama *et al.* [7] measured the thickness of the oil film in the piston ring under actual operating conditions in a diesel engine. Their results showed that the thickness agreed well with the hydrodynamic lubrication theory if oil was adequately supplied. Takiguchi *et al.* [13] have developed a method for simple simultaneous measurements of oil film thickness in piston rings at plural points of internal combustion engines using laser-induced fluorescence. They found that the difference in oil film thickness is attributed to the difference in the amount of lubricating oil supplied to the oil ring, and the effect is greater than that caused by engine speed or load. As mentioned above, the measured film thickness more strongly supported the hydrodynamic lubrication theory if oil was adequately supplied at high engine speeds.

In recent years, inverse models [16, 17] have been widely applied to many design and manufacturing problems in which some of the surface conditions cannot be measured. In this methodology, the boundary conditions are unknown and can be represented in a form of polynomial function with undetermined coefficients. By using the least-square error method, system equations can be constructed to solve the undetermined coefficients. Cheng and Chang [2] adopted a conjugate gradient method to explore optimizing the profile of the slider surface in hydrodynamic lubrication. The specified load demands considered in their study are categorized into two kinds: (1) specified pressure distribution within the fluid film, and (2) specified resultant forces plus specified centers of load. However, in the literature, the inverse method has rarely been applied to problems concerning piston ring profile. In this paper, the idea of an inverse model is proposed to estimate the piston ring profile and pressure distribution. The proposed algorithm only needs to obtain the load and boundary conditions of the piston ring to estimate the profile and the pressure distribution.

II. THE ORETICAL ANALYSIS

1. Governing Equation

The piston ring geometry and the coordinate system are shown in Fig. 1. It is assumed that the lubricating surfaces of piston ring and cylinder liner are all smooth and the two surfaces are separated by oil film at all time in the lubrication region. Therefore, the Reynolds equation is applicable throughout the engine cycle. Circumferential effects are neglected, which enables the problem to be reduced to an axial symmetrical problem. The viscosity and density are assumed to be pressure independent. Then, under the usual assumptions for the hydrodynamic lubrication, the steady state one-dimensional Reynolds equation is

$$\frac{\partial}{\partial x}=(\frac{\rho h^3}{\eta}\frac{\partial p}{\partial x})=6u_b\frac{\partial(\rho h)}{\partial x} \tag{1}$$

where u_b represents the piston velocity. Eq. (1) can be integrated as:

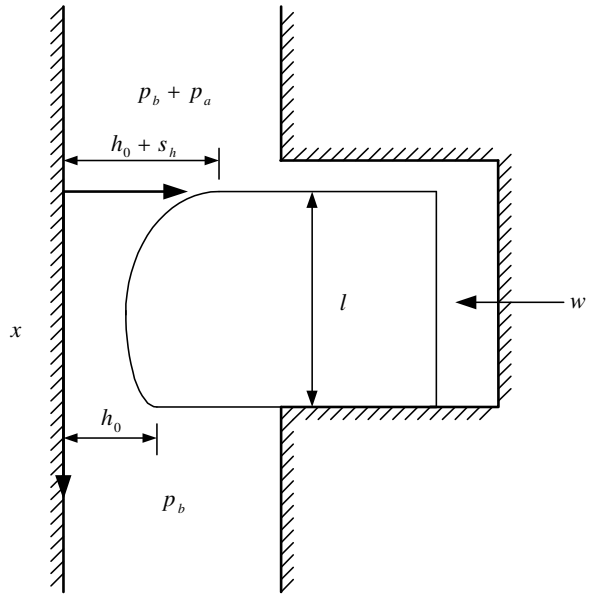

Fig. 1. A schematic of piston ring and cylinder bore conjunction.

$$\frac{dp}{dx}=6\eta u_b\frac{h-h_m}{h^3} \tag{2}$$

where h_m is the film thickness at maximum pressure, i.e. $dp/dx=0$. The dimensionless form of Eq. (2) is

$$\frac{dP}{dX}=6\frac{H-H_m}{H^3} \tag{3}$$

The boundary conditions for Eq. (3) are:

$$P=P_b+P_a \text{ , at } X=X_{in}(=0) \tag{4a}$$

$$P=P_a \text{ , at } X=X_{end}(=1) \tag{4b}$$

The load-carrying capacity of the oil film per unit length is:

$$w=\int_0^l p dx \tag{5}$$

The pressure acting on the piston ring in the radial direction is assumed to be composed of the pressure at the inner side of the ring and the piston ring elastic pressure. Therefore, the dimensionless load balance equation for the piston ring is given as:

$$W=\int_0^1 PdX=P_g+P_e \tag{6}$$

2. Inverse Algorithm for Estimate Piston Ring Profile and Pressure Distribution

Once the film thickness is given, the pressure distribution can be calculated directly by solving Eq. (3) using iteration method, and then the force acting on piston ring can be given by integrating the pressure distributions. The solution is referred to the 'numerical' solution. However, piston ring profile is unknown in advance nor is the film thickness. In order to obtain a piston ring profile, the film thickness distribution can be represented in the

form of polynomial with inlet/outlet conditions satisfied, i.e.

$$H_k = (X_k - 1)\sum_{j=1}^{m+1} C_j X_k^j - X_k + (H_0 + 1) \quad (7)$$

where C_j is an undetermined coefficient and m is a positive integer. In this equation, H_k is the film thickness at X_k with n_p chosen points. Note that at $X = 0$, Eq. (7) can be simplified to $H = H_0 + 1$, and at $X = 1$, Eq. (7) can be simplified to $H = H_0$.

The pressure distribution can also be represented in the polynomial function with boundary conditions satisfied, i.e.

$$P_k = (X_k - 1)\sum_{i=1}^{n+1} B_i X_k^i - X_k P_a + (P_b + P_a) \quad (8)$$

where B_i is an undetermined coefficient and n is a positive integer. Note that at $X = 0$, Eq. (8) can be simplified into $P = P_b + P_a$, and at $X = 1$, Eq. (8) can be simplified into $P = P_b$.

Substituting Eq. (8) into Eq. (6), the force balance equation becomes

$$W = (P_b + \frac{1}{2}P_a) - \sum_{i=1}^{n+1} \frac{1}{(i+1)(i+2)} B_i \quad (9)$$

Substituting Eqs. (7) and (8) into Eq. (3), the governing equation becomes

$$\left\{-P_a + \sum_{i=1}^{n+1}[X_k^{(i-1)}(2X_k - 1) + (i-1)X_k^{(i-2)}(X_k^2 - X_k)]B_i\right\} [(X_k - 1)\sum_{j=1}^{m+1} C_j X_k^j - X_k + (H_0 + 1)]^3 = 6\left\{[(X_k - 1)\sum_{j=1}^{m+1} C_j X_k^j - X_k + (H_0 + 1)] - H_m\right\} \quad (10)$$

In order to simplify calculation, Eq. (10) can be rewritten as:

$$f_k = \left\{-P_a + \sum_{i=1}^{n+1}[X_k^{(i-1)}(2X_k - 1) + (i-1)X_k^{(i-2)}(X_k^2 - X_k)]B_i\right\} H_{kb}^3 - 6\left\{[(X_k - 1)\sum_{j=1}^{m+1} C_j X_k^j - X_k + (H_0 + 1)] - H_m\right\} \quad (11)$$

where H_{kb} is the value of film thickness in the forward iteration.

It is obvious that the estimated film thickness and pressure are different from the numerical ones. Hence, to obtain the smallest error between the numerical and estimated values, the least-square error method and variational method are employed here subject to the force balance constraint. The least-square error method and variational method require the residual function to be minimized.

$$\frac{\partial G}{\partial B_i} = 0, \ i = 1, 2, 3, \cdots, n+1 \quad (12)$$

$$\frac{\partial G}{\partial C_j} = 0, \ j = 1, 2, 3, \cdots, m+1 \quad (13)$$

where the residual function with Lagrange multiplier λ is

$$G = \sum_{k=1}^{n_p} f_k^2 + \lambda[W - (P_b + \frac{1}{2}P_a) + \sum_{i=1}^{n+1} \frac{1}{(i+1)(i+2)} B_i] \quad (14)$$

Eqs. (12) and (13) can be rewritten as:

$$\sum_{k=1}^{n_p} \beta_{ik}\alpha_k + \frac{0.5}{(i+1)(i+2)}\lambda = \sum_{k=1}^{n_p} \beta_{ik}\xi_k, \ i = 1, 2, 3, \cdots, n+1 \quad (15)$$

$$\sum_{k=1}^{n_p} \gamma_{jk}\alpha_k = \sum_{k=1}^{n_p} \gamma_{jk}\xi_k, \ j = 1, 2, 3, \cdots, m+1 \quad (16)$$

where

$$\beta_{ik} = [X_k^{(i-1)}(2X_k - 1) + (i-1)X_k^{(i-2)}(X_k^2 - X_k)]H_{kb}^3 \quad (17)$$

$$\gamma_{jk} = -6X_k^j(X_k - 1) \quad (18)$$

$$\xi_k = 6[(H_0 + 1) - X_k - H_m] + P_a H_{kb}^3 \quad (19)$$

$$\alpha_k = \sum_{i=1}^{n+1}[X_k^{(i-1)}(2X_k - 1) + (i-1)X_k^{(i-2)}(X_k^2 - X_k)]H_{kb}^3 - \sum_{j=1}^{m+1} 6X_k^j(X_k - 1) \quad (20)$$

The unknowns B_i, C_j and λ can be solved by the $n+m+3$ equations. Furthermore, Eqs. (9), (15) and (16) can be rearranged in the following matrix equation:

$$\mathbf{\Psi}_{(n+m+3)\times(n+m+3)}\mathbf{\Lambda}_{(n+m+3)\times 1} = \mathbf{\Phi}_{(n+m+3)\times 1} \quad (21)$$

The components of Ψ(n+m+3)×(n+m+3) are X and H. The components of Λ(n+m+3) ×1 are B_i, C_j and λ, and the components of Φ(n+m+3) ×1 are boundary terms and operation conditions, i.e. X, H_0, H_m, P_a, P_b and W. The Gauss-Seidel method and Newton-Raphson method are employed to solve Eq. (21) iteratively. The estimated film thickness and pressure can be calculated from Eqs. (7) and (8), respectively, after the unknown variables B_i, C_j and λ are solved. The flow chart for the solution procedure is shown in Fig. 2.

III. RESULT AND DISCUSSION

1. Numerical Solution

In order to illustrate the validity of the present technique as discussed above, some "target" values must be given. First, the film thickness must be given. Then, using the finite difference method with 101 grid points, the Gauss-Seidel iteration is employed to calculate the numerical solution of the pressure distribution, as well as the load and friction coefficient under the conditions of $P_b = 0.2$, $P_a = 0.4$ and $H_0 = 1.0$. This problem is referred to as a direct problem and the solution is called the "numerical" solution. This numerical solution is taken as the reference film thickness and pressure distribution between the piston ring and the cylinder liner under fully flooded lubrication conditions. In this paper, the "numerical" solution is treated as the "target" value, and the film thickness is treated as the piston

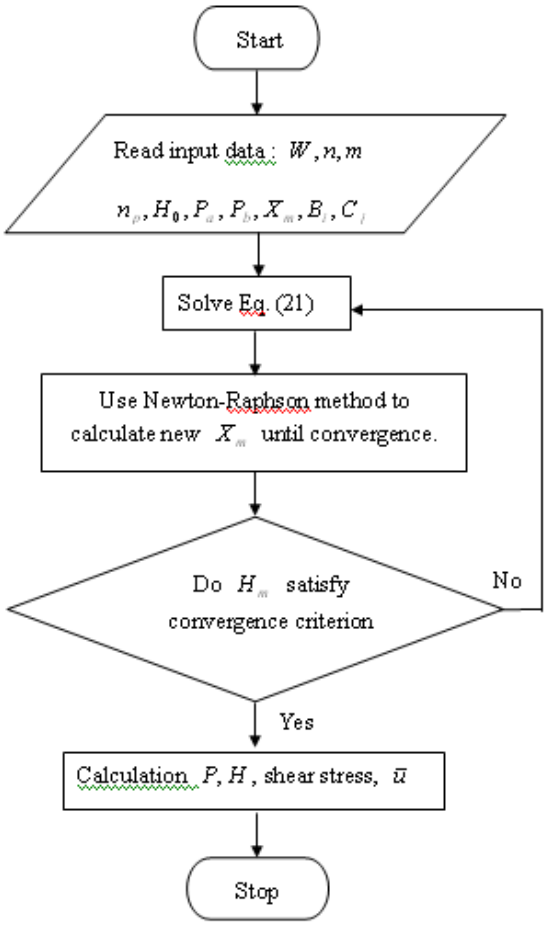

Fig. 2. Flow diagram of computational procedure.

ring profile.

Under the conditions of $H = H_0 + 1 - X$, $P_b = 0.0$, $P_a = 0.0$, and $H_0 = 1.0$, Hamrock [8] solved the integrated form of the Reynolds equation for a fixed-incline slider bearing as expressed in Eq. (3) to obtain a "closed form solution" as:

$$P = \frac{6X(1-X)}{(H_0 + 1 - X)^2 (1 + 2H_0)} \tag{22}$$

Note that the dimensionless pressure is a function of X and H_0. The variation in P with X for various values of H_0 is shown in Fig. 3. As can be seen, the numerical results of P with X for various values H_0 obtained by the proposed algorithm are in good agreement with those obtained by Hamrock [8] with 101 grid points.

As seen in Fig. 4, the piston ring profile is different, and the pressure distribution and load-carrying capacity of film thickness also show discrepancies. Curves C and D have a similar manufactured profile function; however, their slopes are different, so the pressure distributions are different. The greater the wedge-profiled effect is, the higher the pressure in the inlet and central areas, and the lower smaller the pressure in the exit area.

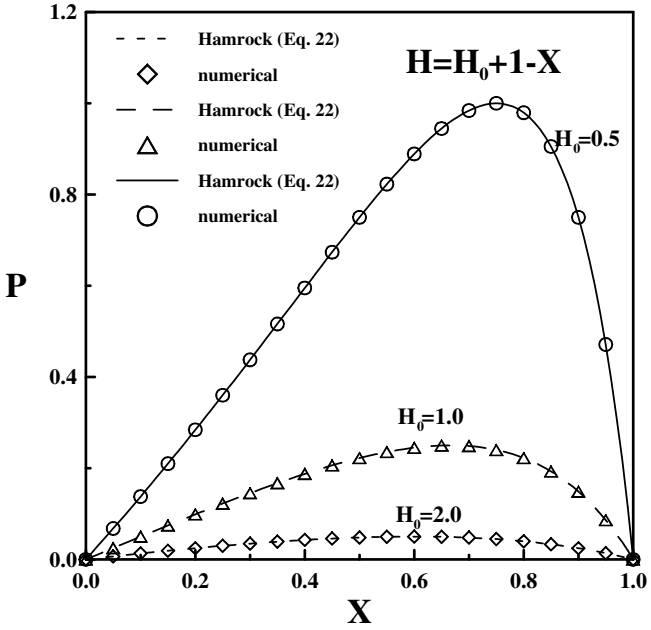

Fig. 3. Comparison between numerical results of P with X for various values of H_0 estimated by the present algorithm and those obtained by Hamrock [8].

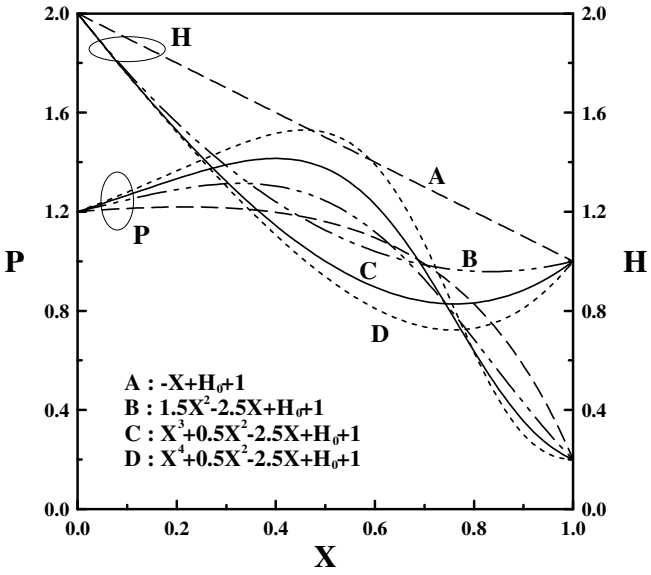

Fig. 4. Pressure distributions with different piston ring profiles.

In addition, the load-carrying capacity of film thickness is also greater. The degree of the polynomial function employed to describe the piston ring profile has some influence on pressure distribution, as well as the load and friction coefficient. Figure 5 shows that the greater the value of m, that is, the degree of the polynomial function used for the piston ring profile (with all $C_j = 1.0$ in Eq. (7)), the greater the maximum pressure, load and friction coefficient, and the smaller the minimum film thickness are.

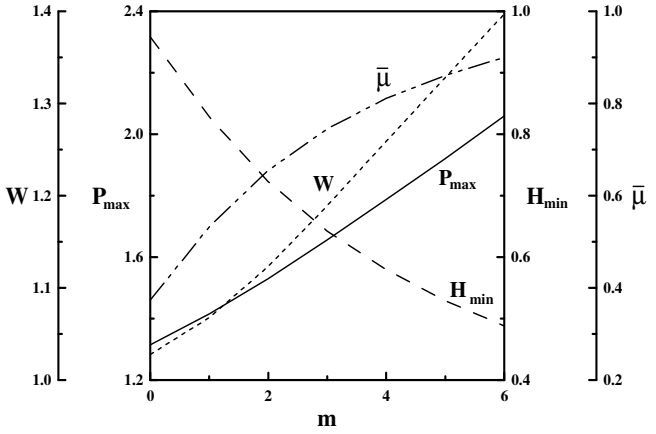

Fig. 5. Maximum pressure, minimum film thickness, load, and friction coefficient versus m.

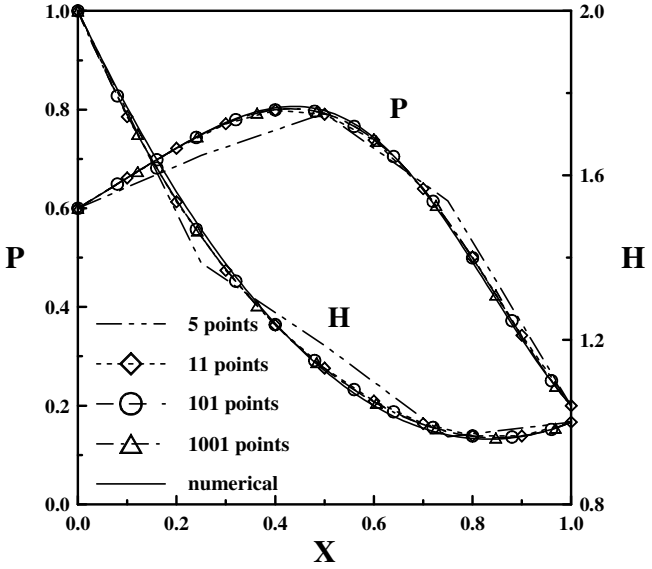

Fig. 6. Pressure distributions and film profiles estimated by the present algorithm with different number of points in film thickness.

2. Inverse Solution for Piston Ring Profile and Distribution Pressure

The pressure distributions and film thicknesses estimated by the present algorithm are plotted and compared with that obtained from numerical solutions as shown in Figs. 6-8. Several numerical tests have been performed. Typical results for the case of $W = 0.6379$, $P_b = 0.2$, $P_a = 0.4$, $H_0 = 1.0$, $X_m = 0.44$, $P_m = 0.8064$, $X_{\min} = 0.83$, and $H_{\min} = 0.9584$ with 101 grid numbers are shown in Figs. 6-8. The unknown pressure distribution is approximated by a polynomial function of degree 5 (Eq. (8) with n = 3), and the unknown film thickness is approximated by a polynomial function of degree 4 (Eq. (7) with m = 2). The number of grid points in the film can be 5, 11, 101, and 1001 on a domain from Xin =0 to Xend =1.0 with uniform mesh. After the coefficients of the polynomial functions are solved from Eq. (21), the estimated film thickness and pressure distribution can be calculated from Eqs. (7) and (8), respectively. Figure 6 shows that the number of grid points significantly influences film thickness and pressure distribution. As the grid points increase, the solution of film thickness and pressure distribution approaches the numerical solution. Eleven grid points in the film thickness give a fairly accurate estimated solution of film thickness and pressure distribution, but there is still a very small error compared with numerical solution. For the film with 101 grid points, the solution of film thickness and pressure distribution are almost identical to the numerical solution.

3. Errors Effect on Inverse Solution

Figure 2 shows that the input parameters are W , n , m , n_p , H_0 , P_a , P_b , X_m , B_i , and C_j in the beginning of the iteration. In the above Figs. 6 and 7, the effects of the degree of the polynomial function and the number of grid points on a domain from Xin =0.0 to Xend =1.0 with uniform mesh have been discussed. In the initial guess, all B_i are set to be zero. The initial guessed values of B_i have no significant effects on the result of the estimated film thickness and pressure distribution. However, the initial guessed values of C_j and X_m have significant effects upon the estimated results. Hence, the next step is to investigate how the variations in initial guesses (C_j and X_m) affect the estimated film thickness and pressure distribution. Figure 8 shows the effects of the initial guessed value of X_m on film thickness and pressure distribution. As can be seen, when the initial guess is smaller than its numerical value ($X_m = 0.44$), the estimated film thickness is larger than its numerical value, and the estimated pressure distribution is smaller than its numerical value around the $X < 0.6$ region. In addition, to satisfy the force balance equation, the pressure distribution is larger than its numerical value around the $X > 0.6$ region. Moreover, when the initial guess is larger than its numerical value, the estimated film thickness is smaller than its numerical value, and the estimated pressure distribution is larger than its numerical value around the $X < 0.6$ region, and the estimated pressure distribution is smaller than its numerical value around the $X > 0.6$ region. Table 1 shows that the initial guessed value of X_m is 0.44, the errors associated with X_m , $P_{\max}$, $X_{\min}$, $H_{\min}$, and $\bar{\mu}$ are -2.3% , -0.63%, 2.41%, 0.41%, and -0.67%, respectively. When the initial guessed value of X_m is 0.352, that is, the variation in initial guessed value of X_m is –20.0%, then the error associated with $P_{\max}$ is -3.96%, and the error associated with $H_{\min}$ is 4.35%. When the initial guessed value of X_m is 0.528, that is, the variation initial guessed value of X_m is 20.0%, then the error associated with $P_{\max}$ is 1.98%, and the error associated with $H_{\min}$ is –5.07%. Hence, when the error of the initial guessed value of X_m is

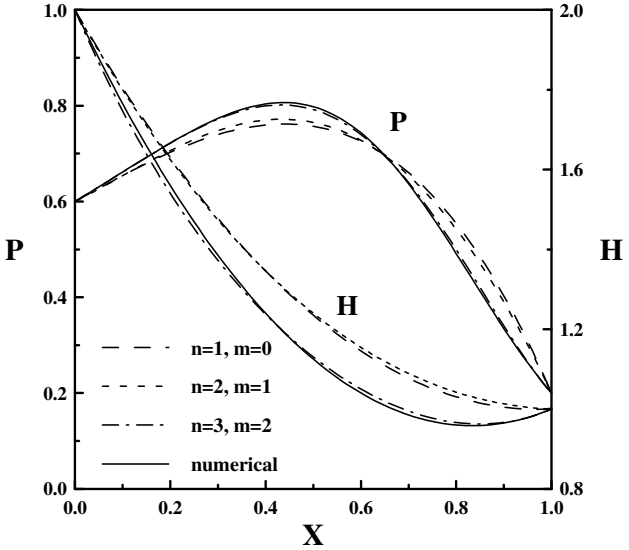

Fig. 7. Pressure distributions and film profiles estimated by the present algorithm with different degrees of the polynomial function.

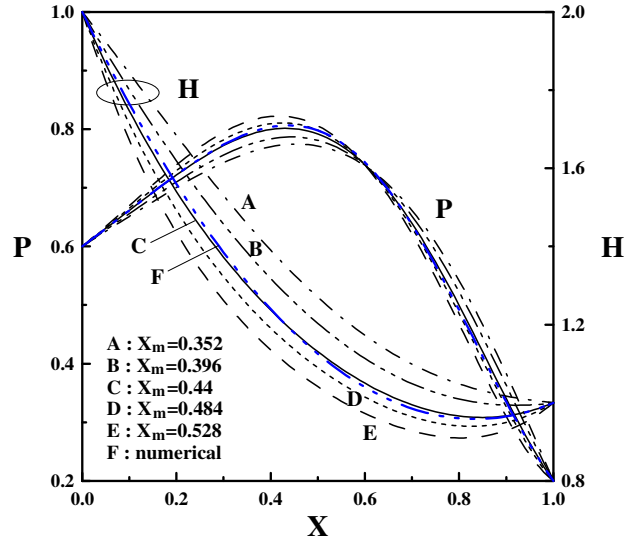

Fig. 8. Effect of error in X_m on pressure distributions and film profiles.

between –20.0% and 20%, the error associated with P_{max} is within 4.0%, and the error associated with H_{min} is within 5.0% as obtained by the present algorithm.

The initial guessed values of C_j are all zero except for C_1. Table 2 shows that the initial guessed value of C_1 is 1.5, and the errors associated with X_m, P_{max}, X_{min}, H_{min}, and $\bar{\mu}$ are -2.3%, -0.63%, 2.41%, 0.41%, and -0.67%, respectively. When the initial guessed value of C_1 is 1.0, that is, the variation in initial guessed value of C_1 is -33.33%, then the error associated with P_{max} is -3.99%, and the error associated with H_{min} is 4.35%. When the initial guessed value of C_1 is 1.8, that is, the variation in initial guessed value of C_1 is 20.0%, then the error associated

Table 1. Effect of error of the initial guessed value of X_m on minimum film thickness, maximum pressure, and friction coefficient (The superscript p represent present, the superscript n represent numerical).

Item \ X_m	0.352	0.396	0.44	0.484	0.528
$(X_m^p - X_m^n)/X_m^n(\%)$	4.5	0.0	-2.3	-4.5	-4.5
$(P_{max}^p - P_{max}^n)/P_{max}^n(\%)$	-3.96	-2.46	-0.63	0.51	1.98
$(X_{min}^p - X_{min}^n)/X_{min}^n(\%)$	20.48	10.84	2.41	0.0	-3.61
$(H_{min}^p - H_{min}^n)/H_{min}^n(\%)$	4.35	3.65	0.41	-1.96	-5.07
$(\bar{\mu}^p - \bar{\mu}^n)/\bar{\mu}^n(\%)$	-12.76	-7.35	-0.67	3.57	9.02

Table 2. Effect of error of the initial guessed value of C_j on minimum film thickness, maximum pressure, and friction coefficient (The superscript p represent present, the superscript n represent numerical).

Item \ C_1, ($C_2 = 0.0$)	1.0	1.2	1.5	1.8	2.0
$(X_m^p - X_m^n)/X_m^n(\%)$	4.55	2.27	-2.3	-4.54	-6.82
$(P_{max}^p - P_{max}^n)/P_{max}^n(\%)$	-3.99	-2.74	-0.63	1.84	3.68
$(X_{min}^p - X_{min}^n)/X_{min}^n(\%)$	20.48	13.25	2.41	-2.41	-4.82
$(H_{min}^p - H_{min}^n)/H_{min}^n(\%)$	4.35	4.00	0.41	-4.72	-8.61
$(\bar{\mu}^p - \bar{\mu}^n)/\bar{\mu}^n(\%)$	-12.95	-8.40	-0.67	8.44	15.38

with P_{max} is 1.84%, and the error associated with H_{min} is –4.72%. Hence, when the error of the initial guessed value of C_1 is between –33.33% and 20%, the error associated with P_{max} is within 4.0%, and the error associated with H_{min} is within 5.0% as obtained by the present algorithm. As mentioned above, the initial guessed values of X_m and C_1 have significant effects on the estimated P_{max} and H_{min}. It is obvious that the present algorithm gives a very good approach on estimated P_{max} and H_{min} values, but it is still limited by the initial guess.

IV. CONCLUSION

This paper used an inverse method to design the piston ring profile. The proposed algorithm needs only to obtain the load and boundary conditions of the piston ring to estimate the profile and the pressure distribution. In order to demonstrate the capability of the present algorithm, a number of test cases are conducted. The effects of the design parameters of the piston

ring and the characteristics of this algorithm were discussed. The results are summarized as follows.

(1) The greater the degree of the polynomial function used, the greater the maximum pressure, as well as the load and friction coefficient are, and the smaller the minimum film thickness is.

(2)With an increase in the degree of the polynomial and the number of grid points, the errors in the estimated piston ring profile and pressure distribution can be reduced. The estimated values can be approximated accurately by $n = 3$ and $m = 2$.

(3) C_j and X_m have more obvious effects upon the present algorithm. When the error of the initial guessed value of X_m is between –20.0% and 20%, and the error of the initial guessed value of C_1 is between –33.33% and 20%, then the error associated with $P_{\max}$ is within 4.0%, and the error associated with $H_{\min}$ is within 5.0% as estimated by the present algorithm. Thus, the initial guessed value of C_j can allow greater error than that of X_m.

ACKNOWLEDGEMENTS

The authors would like to express their appreciation to the National Science Council (NSC-95-2221-E-132-003) in Taiwan for financial support.

REFERENCES

1. Castleman, R. A., "A Hydrodynamic Theory of Piston Lubrication," *Physical Review*, Vol. 7, pp. 364-367 (1936).
2. Cheng, C. H. and Chang, M. H., "Profile Design for Surface of a Slider by Inverse Method," *ASME J. of Tribology*, Vol. 126, pp. 519-526 (2004).
3. Dowson, D., Economou, P. N., Ruddy, B. L., Strachan, P. L. and Baker, A. J. S., "Piston Ring Lubrication-Part II, Theoretical Analysis of a Single and a Complete Ring Pack," *Proc. of Energy Conservation Through Fluid Film Lubrication Technology-Frontier in Research and Design*, pp. 23-51 (1979).
4. Dowson, D., Ruddy, B. L. and Economou, P. N., "The Elastohydrodynamic Lubrication of Piston Rings," *Proc. Roy. Soc.*, A386, pp. 409-430 (1983).
5. Eilon, S. and Saunders, O. A., "A Study of Piston Ring Lubrication," *Proc. Instn. Mech. Engrs.*, Vol. 171, pp. 427-433 (1957).
6. Furunama, S., "A Dynamic Theory of Piston Ring Lubrication," *Bulletin of the JSME, first report-calculation*, Vol. 2, pp. 423-428 (1959). *Second report-experiment*, Vol. 3, pp. 291-297 (1960). *Third report-measurement of oil film thickness*, Vol. 4, pp. 744-752 (1961).
7. Furuhama, S., Asahi, C., and Hiruma, M, "Measurement of Piston Ring Oil Film Thickness in an Operating Engine," *ASLE Trans.*, Vol. 26, No. 3, pp 325-332 (1983).
8. Hamrock, Bernard J, *Fundamentals of Fluid Film Lubrication*, McGRAW-HILL International editions, 1994.
9. Hawkes, C. J. and Hardy, G. F., "The Friction of Piston Rings," *Trans. N.E. Coast Inst. Engrs. And Shipbuilders*, Vol. 52, pp. 143 (1936).
10. Hwu, C. J. and Weng, C. I., "Elastohydrodynamic Lubrication of Piston Rings," *Wear*, Vol. 151, pp. 203-215 (1991).
11. Jeng, Y. R., "Theoretical Analysis of Piston-Ring Lubrication Part I-Fully Flooded Lubrication," *Tribology Transactions*, Vol. 35, No. 4, pp. 696-706 (1992).
12. Takiguchi, M., Machida, K. and Furuhama, S., "Piston Friction Force of a Small High Speed Gasoline Engine," *ASME J. of Tribology*, Vol. 110, pp. 112-119 (1988).
13. Takiguchi, M., Nakayama, K, Furuhama, S, and Yoshida, H., "Variation of Piston ring Oil Film Thickness in an Internal Combustion Engine," *SAE Paper* 980563 (1998).
14. Ting, L. L. and Mayer, J. E., Jr, "Piston Ring Lubrication and Cylinder Bore Wear Analysis, Part I-Theory, Part II-Theory Verification," *ASME Journal of Lubrication Technology*, Vol. 96, No. 2, pp. 258-266, Vol. 96, No. 3, pp. 305-314 (1974).
15. Wu, G. M. and Chen, Z. X., "The Numerical Study of Piston Ring Elastohydrodynamic Lubrication by the Multigrid Method," *Tribology Transactions*, Vol. 35, No. 1, pp. 135-141 (1992).
16. Yang, C. Y., "A Linear Inverse Model for the Temperature-Dependent Thermal Conductivity Determination in One-Dimensional Problems," *Applied Mathematical Modelling*, Vol. 22 pp. 1-9 (1998).
17. Yang, C. Y. and Chen, C. K., "The Boundary Estimation in Two-Dimensional Inverse Heat Conduction Problems," *Journal of Physics D: Applied Physics*, Vol. 29 pp. 333-339 (1996).

NOMENCLATURE

B_i	coefficient in Eq. (8)
C_j	coefficient in Eq. (7)
h	film thickness (m)
hm	film thickness when $dp/dx = 0$ (m)
H	dimensionless film thickness, h/s_h
H_0	dimensionless outlet film thickness, h_0/s_h
l	length in x direction (m)
p	pressure (Pa)
p_a	discrepancy of pressure between inlet and outlet (Pa)
p_b	pressure at outlet (Pa)
P	dimensionless pressure, $ps_h^2/\eta u_b l$
P_e	dimensionless piston ring elastic pressure, $p_e s_h^2/\eta u_b l$
P_g	dimensionless pressure at the inner side of the piston ring, $p_g s_h^2/\eta u_b l$
s_h	shoulder length (m)
w	load per unit width (N)
W	dimensionless load, $ws_h^2/\eta u_b l^2$
x	coordinate (m)
X	dimensionless coordinate, x/l
X_m	dimensionless value of X when $dp/dx = 0$, x_m/l
λ	Lagrange multiplier
μ	friction coefficient
$\overline{\mu}$	dimensionless friction coefficient, $\mu l/s_h$
ρ	density of lubricant (kg/m^3)